3s photoemission spectra of Fe/Cu(100) films

Kang-Ho Park*

Research Department, Electronics and Telecommunications Research Institute, Yu-Song, P.O. Box 106, Daejon, 305-600, Korea

S.-J. Oh

Department of Physics, Seoul National University, Seoul, 151-742, Korea

K. Shimada, A. Kamata, K. Ono, A. Kakizaki, and T. Ishii

Synchrotron Radiation Laboratory, Institute for Solid State Physics, University of Tokyo, Tokyo 106, Japan

A simple cluster model calculation scheme which successfully describes the line shape and intensity ratio of recent spin resolved Fe 3s spectra of metallic Fe has been developed. From fitting the 3s spectra of bcc-bulk Fe, we found that the configuration interaction effect is important to the understanding of the 3s spectra. This model was applied to the Fe 3s spectra obtained from the ultrathin [0.7, 1.7, and 2 monolayer (ML)] Fe overlayers on Cu(100), and the 3s spectra of thin films were described well within our cluster model framework. Indeed the difference between the Fe 3s spectra of ultrathin films and bulk-bcc Fe was found to be consistent with the fact that the local magnetic moment of ultrathin films is smaller than that of the bcc bulk in our model. However, we did not find significant changes of the experimental 3s spectra between 0.7-, 1.7-, and 2-ML-thin films, which means that local magnetic moments of thin films do not change much below 2 ML.

I. INTRODUCTION

The advanced technology of producing and probing ultrathin magnetic films provides interesting opportunities to investigate magnetic properties of artificial crystalline materials. Indeed epitaxially grown magnetic materials (Cr, Mn, Fe, Co, and Ni on noble metals) have been a current issue for two-dimensional (2D) magnetism and metastable crystalline phases like fcc iron.[1,2] In the ultrathin magnetic films, because several conditions likes crystal structure, lattice constant, substrate effect, and 2D effect[3,4] can be controlled, more opportunities for the understanding of magnetism can be provided. This is one reason why many researchers study ultrathin magnetic films. The difficulty of magnetism arises from its quantum mechanical property and many body effect. Until now ground state magnetic properties of Fe and Ni have been described within itinerant electron magnetism like Stoner model, although lots of magnetic properties of finite temperature such like Curie temperature, the magnitude of local moment, and short range magnetic order above Curie temperature in magnetic transition metals remain unsolved.

Of the ultrathin magnetic films, Fe on Cu(100) has been an interesting system due to its distinct magnetic property. It has fcc Fe structure similar to the γ-phase fcc bulk iron, with lattice constant a_0(3.61 Å) comparable to 3.59 Å of bulk γ phase.[1] But its magnetic property is extremely different from that of bulk γ phase. While bulk fcc iron is known to have antiferromagnetic ground state from band calculation results,[5] ultrathin fcc film shows ferromagnetic property with various Curie temperature depending on the thickness.[6,7] And usually the easy magnetic axis is perpendicular to the sample structure.[8] These properties have been found from a number of experimental techniques like SMOKE (surface magneto-optic Kerr effect),[6,7] SPPE (spin polarized photo emission),[9] LEED (low energy electron diffraction),[10] XPD (x-ray pho-

toelectron diffraction),[11] RHEED (reflection high energy electron diffraction),[12] and SEMPA (scanning electron microscopy with polarization analysis).[8] Its growth mode has also been an interesting problem. It is now generally accepted that the film grows forming a 3D island up to 2 ML (monolayer) as Volmer-Weber growth mode, and above 2 ML it is converted to the layer-by-layer growth mode (Frank-van der Merwe) (Ref. 12) at room temperature. Usually ferromagnetism appears near 2 ML, and the maximum Curie temperature occurs at 3–4 ML, and above 10 ML layer-by-layer growth mode fails and the bcc structure Fe growth appears.[7] Generally the enhancement of magnetic moments in various ultrathin magnetic films has been reported from band calculations,[3,4] and the presence of ferromagnetism in 1–2 ML Fe on Cu(100) was also predicted by band calculation.[13] The reason why ferromagnetism appears at Fe on Cu(100) system has been discussed in various ways. One candidate is the slight increase of the lattice constant and another one is the surface 2D effect. The fact that the magnetic moment of fcc iron depends sensitively on the lattice constant was found from Bagayoko and Callaway's band calculation,[5] and in a 2D system the small coordination number is generally believed to have an effect on the magnetic moment.[4] The origin of various magnetic properties in Fe on Cu(100) system has been also discussed from the viewpoint of surface morphology and interdiffusion by many authors recently.[14,15] But the detailed information of magnetic and electronic property like local magnetic moment and itinerant character has not been understood well. To address this issue, we measured 3s spectra on ultrathin Fe films on Cu(100) with thickness of 0.7, 1.7, and 2 ML. The 3s spectra are interesting because these spectra can provide information about the local electronic and magnetic configuration. Because the radius of 3s orbital in Fe is smaller than 1 Å, the 3s core hole interacts with localized 3d electrons through

Coulomb direct and exchange interaction.

Since the first observation[16,17] of splittings of 3s photoemission spectra of the late transition metal compounds, a number of works about Mn, Fe, Co 3s spectra have been done.[18–22] From the viewpoint of atomic multiplet scheme, the splittings are due to the exchange interaction J between 3s core electron and 3d valence electrons. From this exchange interaction, two spin momentum final state, $S+1/2$ and $S-1/2$ would be possible, where S is the spin of outer 3d electron configuration. The energy separation between these two spin final states should be $J(S+1/2)$, and the intensity ratio is $S+1:S$ according to the Van Vleck theorem.[19] Until recently the overall trends of 3s splittings in Mn, Fe, Co compounds have been described by this exchange splitting scheme. But detailed investigations gave inconsistent results. Several years ago van Acker *et al.*[20] collected extensive data on Fe 3s splitting of various compounds, and showed poor correlation between the 3s exchange splitting and Fe local moment. This inconsistency seems to arise from the configuration interaction effect due to the delocalized property of 3d electron and the final state screening. The evidence of configuration interaction effect could be found easily. In Ni metal small satellite in the 3s spectra was interpreted as a formation of an atomic two hole bound state. In this case d electrons on a given site can have final d^9 or d^{10} configuration. The main peak has the fully screened d^{10} configuration, while the satellite peak has the unscreened d^9 configuration. Recently Oh, Gweon, and Park[21] described 3s splitting of various late transition metal ionic compounds as a combination of the exchange splitting including atomic configuration mixing effect and the charge transfer satellites arising from the hybridization between 3d and ligand valence band. Their model would be useful for ionic or covalent compounds, but it is not suitable for metallic compounds. For metallic systems Kakehashi and co-workers[22] calculated 3s core spectra using projection operator method within the tight-binding model considering 3s-3d exchange interaction. They considered the itinerant character of outer 3d electron in describing 3s core spectra, so their work made a significant contribution to the understanding 3s core level splittings in metallic compounds. But because the 3d band was simplified to a single s band, it has difficulty in describing the real data, where spin state of 3d electrons is important.

II. CLUSTER MODEL CALCULATION AND BULK bcc Fe 3s SPECTRA

Recently the spin-resolved photoemission of Fe 3s core level[23–25] provided decisive information for the 3s splitting of Fe metal. Overall trends correspond to atomic exchange interaction scheme of $d^8(S=1)$ configuration,[25] but details are significantly different. In the simple atomic model of Fe atom having $d^8(S=1)$ configuration, the majority spin spectrum simply consists of two exchange splitting peaks (doublet and quartet) having the intensity ratio of 2:1, but in the experimental data high binding energy satellites with significant intensity appear. Above all, the width of the majority spin peak is so large, more than 10 eV, and there are fairly strong high binding energy satellites, which cannot be explained by a simple atomic multiplet model. And the minority spin peak has a long tail, which cannot be considered as a
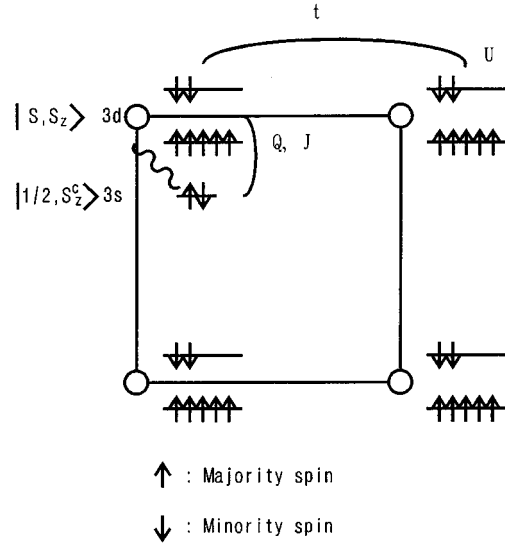
FIG. 1. Four atom cluster model.

Doniach-Šǔnjić type asymmetric line shape. The deviation from the atomic multiplet model reveals the importance of configuration interaction effect of the itinerant 3d system. Without understanding of this many body effect, the magnetic information such as local moment obtained from 3s spectra would include a significant error. In magnetic materials, since an electronic configuration has lots of magnetic ordering configuration, the model calculation of the configuration interaction effect is very difficult. Therefore, in this paper we tried a cluster model calculation with four atom cluster for short range electronic and magnetic configuration in both bulk bcc and ultrathin fcc Fe films.

The model Hamiltonian used to describe 3s photoemission here is five-band Hubbard model including 3s-3d direct and exchange Coulomb interaction,

$$H = H_d + H_c, \qquad (1)$$

$$H_d = \sum_{\langle i,j \rangle} t_{ij} \hat{\Psi}_i^\dagger \hat{\Psi}_j + U \sum_{i,\mu,\nu} n_{i,\mu} n_{i,\nu},$$

$$H_c = -Q \sum_{\sigma,\mu} (1-n_{c,\sigma}) n_\mu - J(SS_c) + \varepsilon_c \sum_\sigma \hat{\Psi}_{c,\sigma}^\dagger \hat{\Psi}_{c,\sigma},$$

where t_{ij} is the hopping integral of 3d electrons with the same spin between i and j sites, U is correlation energy of 3d electrons, Q is direct Coulomb interaction between core 3s and outer 3d electron, and J is exchange interaction between 3s and 3d, μ, ν are orbital and spin indices ranging from 1 to 10 (Fig. 1).

For computational convenience, we consider here only the spin angular momentum of 3d electron at the atomic site. Orbital angular momentum contribution is neglected in this model assuming complete quenching. In our calculation, because only a small size of Fe atom cluster is used, it is impossible to obtain the information on long range magnetic order. So the magnetic moment of the ground state is considered as a model parameter. And the total number of d electrons, total z component of spins, and average local mo-

ment are conserved within the cluster. In the ferromagnetic case, we consider various sets of clusters having possible average local moments from configurations of $3d$ occupation numbers. We assume fully polarized local moment ground state. In the paramagnetic case, we assume fully disordered local moment ground state, and the spin z component of each atom is assumed to have a certain value between $-S$ and S, where S is spin momentum of that atom, but the total sum of z component within the cluster is constrained to be zero. In our model, to take into account the configuration interaction effect the four Fe atom cluster is used to calculate the local electronic configuration with several different short range magnetic ordering. For each magnetic ordering cluster the ground state configuration is obtained by the modified Lanczos method.[26,27]

At first, we obtain Hamiltonian matrix elements of the ground state with the cluster basis. Each cluster basis $|\phi_p\rangle$ is specified by the $3d$ occupation number and the spin configuration for each site,

$$|\phi_p\rangle = |(n_d)_1,(S^2)_1,(S_z)_1\rangle|(n_d)_2,(S^2)_2,(S_z)_2\rangle$$
$$\times |(n_d)_3,(S^2)_3,(S_z)_3\rangle|(n_d)_4,(S^2)_4,(S_z)_4\rangle, \quad (2)$$

where $(n_d)_i$, $(S^2)_i$, and $(S_z)_i$ are the number of $3d$ electrons, the total $3d$ spin momentum, and the total $3d$ z-spin momentum of the i site, respectively. The configuration of these cluster bases depends on the magnetic order. In the ferromagnetic case, possible S and S_z were determined from n_d. But in the paramagnetic case, S depends on n_d, and S_z has a degree of freedom from $-S$ to S.

In the final $3s$ core hole state, we consider $3s$-$3d$ direct Coulomb interaction Q and the exchange interaction J. Final eigenstates are composed of different cluster configuration bases $|\phi_p^f\rangle$,

$$|\psi_p^f\rangle = |(n_d)_1,(S^2)_1,(S_z)_1,s_z^c\rangle|(n_d)_2,(S^2)_2,(S_z)_2\rangle$$
$$\times |(n_d)_3,(S^2)_3,(S_z)_3\rangle|(n_d)_4,(S^2)_4,(S_z)_4\rangle, \quad (3)$$

where s_z^c is the z momentum of the $3s$ core hole spin at the photoionized site.

If the dimension of the final configuration bases is not too large, the exact spectral weight of each final eigenstate can be obtained from the exact matrix diagonalization. But for the large matrix size, an easier calculation method is necessary. We use the Haydock recursion method[28] for $3s$ spectra, because this method is known to give nearly exact simulated spectra by only a few iterations. The spectral function $S(\varepsilon)$ is calculated from the Green function $G(x)$,

$$S(\varepsilon) = -\text{Im}[G(\varepsilon+i0^+)], \quad (4)$$

$$G(x) = \cfrac{1}{x-a_0-\cfrac{b_1}{x-a_1-\cfrac{b_2}{x-a_2-\cdots}}}, \quad (5)$$

where a_n and b_n are as follows ($n=0,1,2,\dots$):
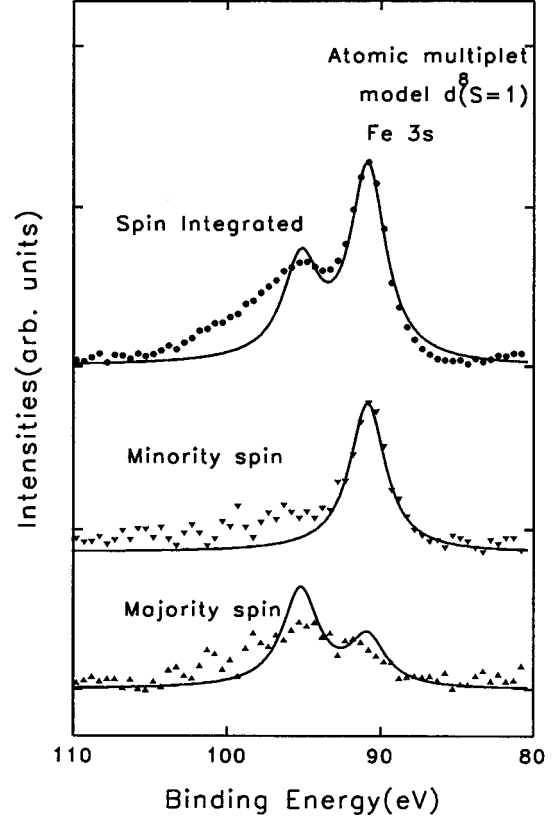
FIG. 2. Hillebrecht *et al.*'s $3s$ spin resolved experimental spectra (Ref. 24) compared with simple atomic d^8 configuration model. The dots and solid lines indicate experiment and theory, respectively.

$$|\psi_0^f\rangle = \hat{a}_{3s}|\psi_G\rangle, \quad (6)$$

$$a_n = \frac{\langle\psi_n^f|H|\psi_n^f\rangle}{\langle\psi_n^f|\psi_n^f\rangle},$$

$$|\psi_{n+1}^f\rangle = H|\psi_x^f\rangle - a_n|\psi_n^f\rangle - b_n|\psi_{n-1}^f\rangle,$$

$$b_{n+1} = \frac{\langle\psi_{n+1}^f|\psi_{n+1}^f\rangle}{\langle\psi_n^f|\psi_n^f\rangle}.$$

We fitted the recent spin resolved experimental data by our cluster model calculation of the ferromagnetic ground state. In Hillebrecht, Jungblut, and Kisker's[24] experimental data, the minority spin spectrum is composed of a single main peak and a long tail, and the majority spin spectrum is roughly composed of two exchange splitted peaks and higher binding energy satellites (Figs. 2 and 3). Although the experimental result does not show a clear feature due to insufficient statistics, broad majority spectrum with the width of nearly 10 eV cannot be understood from the simple atomic picture, as shown in the comparison with the simple atomic model calculation in Fig. 2.

On the other hand, the correspondence between the cluster model and the experiment in the ferromagnetic case is outstanding as can be seen in Fig. 3. In this case, we calculated the theoretical spectra using four atom cluster model
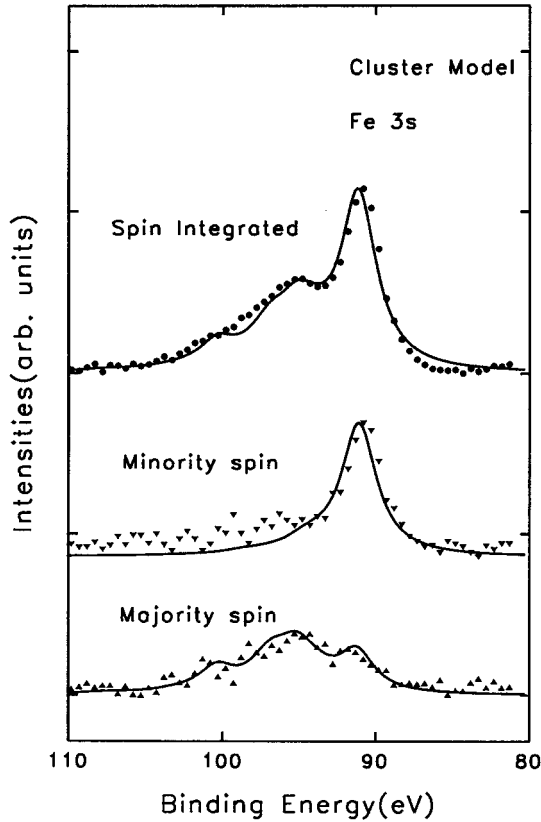
FIG. 3. Hillebrecht *et al.*'s $3s$ spectra (Ref. 24) with cluster model curve. The dots and solid lines indicate experiment and theory, respectively. The fitting parameters are $\bar{S}$, $\bar{S}_z=1.25$, $t=1.1$ eV, $U=3.5$ eV, $J=3.1$ eV, $Q=3.5$ eV.

having 28 d electron configuration, where the average number of $3d$ electrons in each atom is 7. But the average local moment was assumed as 2.5 Bohr magneton, which means that $\bar{S}$ and $\bar{S}_z$ per atom is 1.25. In curve fitting, in order to reduce the arbitrariness in the fitting process, we considered only Lorentzian broadening of $3s$ peaks neglecting Gaussian broadening. The values of model parameters are shown in Table I in detail. They were obtained from the best curve fit, though the potential difficulty in obtaining correct values exist due to many unknown parameters. The correlation energy U of Fe metal has been estimated as 2–3 eV in other papers[29–31] and the bandwidth W of Fe metal was also estimated as 4.5–6 eV.[31] In our model calculation the correlation energy U is 3.5 eV and the d band width resulting from $t=1.1$ eV is 7 eV. These are slightly larger than previous estimated values. However U/W value is reasonably equiva-

TABLE I. The fitting parameters for $3s$ spectra of bulk bcc Fe and fcc Fe thin films (0.7, 1.7, and 2.0 ML [LW: Lorentzian width (FWHM), $(t,U,Q,J,$LW unit: eV)]).

Sample	$\bar{S}$	t	U	Q	J	LW
fcc films	1.0	1.1	3.5	3.5	3.1	1.5
bcc bulk	1.25	1.1	3.5	3.5	3.1	1.4
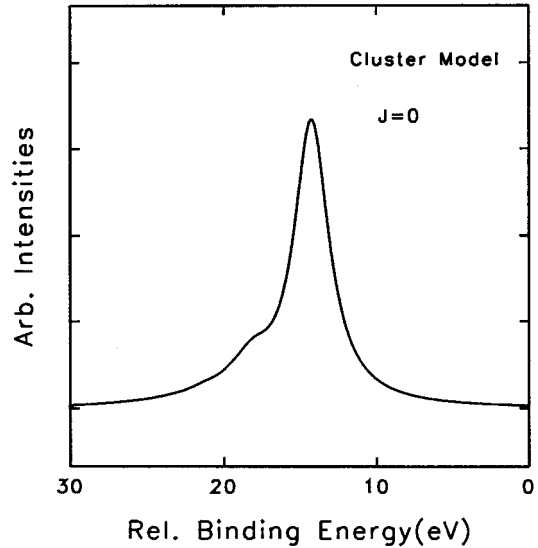
FIG. 4. Simulated spin-integrated spectra with $J=0$. Other fitting parameters are $\bar{S}$, $\bar{S}_z=1.25$, $t=1.1$ eV, $U=3.5$ eV, $J=0.0$ eV, $Q=3.5$ eV.

lent to the previous estimation (~0.5).[31] Considering that these parameters depend on the particular model to describe the electronic structure of metal, the values in Table I can be thought of as reasonable ones. Also the value of the exchange parameter J is about 80% of the atomic Hartree-Fock value,[32] which is reasonable since the intra-atomic Coulomb interactions do not change much between atoms and solids.[30]

The details of spectra could be reproduced by our model calculation. In the majority spin spectra, higher binding energy satellites, and in the minority experimental spin spectra, long tails at higher binding energy side are explained by small satellites in the theoretical calculations. These extra higher binding energy structures arise from the cluster configuration mixing effect. These comparisons show the importance of the configuration interaction effect undoubtedly. The enhancement of the configuration interaction effect in the $3s$ majority spin spectra may seem a little unexpected at first glance, because a similar configuration interaction effect has not been observed in the $2p$ core spectra. It seems that the exchange interaction enhances this configuration interaction peak in the $3s$ majority spin spectrum. From varying exchange interaction J value, we found that the configuration interaction effect profoundly depends on the strength of the exchange interaction. If we set the exchange interaction parameter $J=0$, the spectrum has much reduced satellites as shown in Fig. 4.

In our cluster model, $3s$ spectra of the paramagnetic phase can also be calculated from the ground state configuration of the fully disordered local moment. We calculated the $3s$ spectra of the paramagnetic state with the same parameters as the ferromagnetic case, and the result is shown in Fig. 5. In this figure, the intensity ratio between the main and satellites is prominently different from that of the ferromagnetic ground state. This means that the change of short range magnetic order gives significant change in the $3s$ spectra. This change is due to the condensed matter effect of $3s$
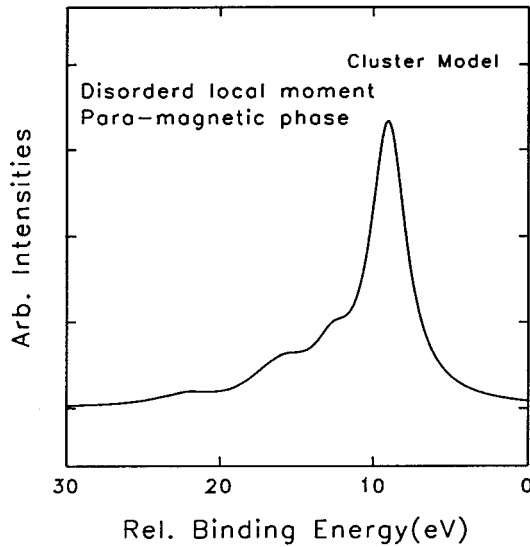
FIG. 5. Calculated $3s$ spectra of paramagnetic phase. The fitting parameters are the same as those of Fig. 3 except total spin $S_z = 0$ in a cluster.

FIG. 6. Comparison of experimental $3s$ spin integrated spectrum of bcc bulk Fe (Hillebrecht et al.'s) with that of fcc Fe 2 ML thin film.

spectra. This result is in contrast to the experimental data, where there is only a slight change below and above Curie temperature,[17] and it implies that Stoner-model–like understanding of the above-Curie temperature phase is not correct. There have been already several suggestions of the local short range magnetic order in the above $-T_c$ phase. Especially from the comparison between the spin resolved photoemission of $3d$ electron and spin resolved calculation in a tight-binding formalism for the bcc iron cluster, a short range magnetic order of at least 4 Å in the vicinity of the Curie temperature[33] has been proposed. Our calculation on the spin resolved $3s$ spectra shows the existence of a similar local short range magnetic order above the Curie temperature.

III. ULTRATHIN Fe FILMS ON Cu(100)

We have measured Fe $3s$ spectra of ultrathin Fe films on the Cu(100) surface. For this experiment, after the mechanical polishing of Cu(100) disk, this substrate was introduced to the sample preparation chamber. In the vacuum of the sample preparation chamber, the clean and ordered Cu(100) surface was prepared by repeated sputtering and annealing. Neon was used for ion bombardments, and beam energy was controlled from 2 kV to 500 V depending on the condition of surface contaminations. The clean and ordered Cu(100) surface was obtained after final 15 minute annealing at 530 °C. We monitored Cu(100) surface by LEED (low energy electron diffraction) and AES (Auger electron spectroscopy). The ultrathin fcc iron films were grown on the clean Cu(100) surface. Iron was evaporated from resistive heating of W wire with a deposition rate of about 1 Å/min. The relative thickness of thin films was obtained from a quartz crystal thickness monitor and calibrated with an Auger spectra signal. During the evaporation, the pressure was maintained below 2×10^{-9} Torr, and the base pressure of the chamber was 2×10^{-10} Torr. In order to measure photoemission spectra,
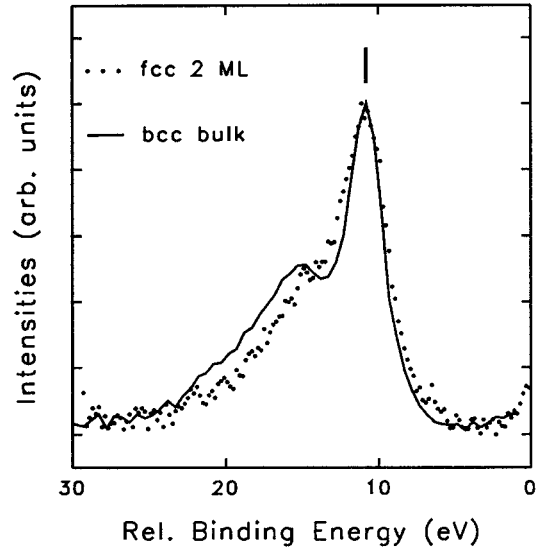
we used BL 19A system of Photon factory at KEK (Japan).[34] In this beamline, strong vuv light from an undulator with the photon energy range 20–250 eV was available as a light source.

We have measured Fe $3s$ photoemission spectra of 0.7, 1.7, and 2 ML ultrathin fcc iron films on Cu(100) with $h\nu = 220$ eV incident light. The $3s$ spectra of various thickness do not exhibit appreciable changes depending on the thickness of fcc ultrathin films. From this fact, we can infer that the local magnetic moment and local short range magnetic-electronic order of fcc thin films are nearly the same at 0.7, 1.7, and 2 ML. It implies that the absence of polarization below 2 ML in other measurements such as SMOKE is not due to the absence of local magnetic moment or short range magnetic order, but probably due to the absence of the long range magnetic order by surface morphology.

In order to compare our results with the bcc bulk, we show Hillebrecht et al.'s $3s$ spin integrated spectra[24] of the bulk iron and those of 2 ML fcc iron in the same figure (Fig. 6). We can see that there are remarkable differences between $3s$ spectra of the bulk and thin films. Although the conditions of experiment and background subtraction are somewhat different for each measurement, we can extract useful information by comparing these two spectra. Neither of the $3s$ spectra can be described within the simple atomic model. It is clear that in both cases the extra higher binding energy satellites appear, which implies that the configuration interaction effect must be taken into account to explain the $3s$ spectra of ultrathin magnetic films as well. Because there are many parameters which influence the structure of Fe $3s$ spectra, an unambiguous analysis is difficult. But it seems reasonable to assume that all intra-atomic parameters like U, Q, and J are the same for these thin films and bulk bcc iron, so we change only the interatomic parameters such as effective hopping integral t and the average spin momentum $\bar{S}$ to
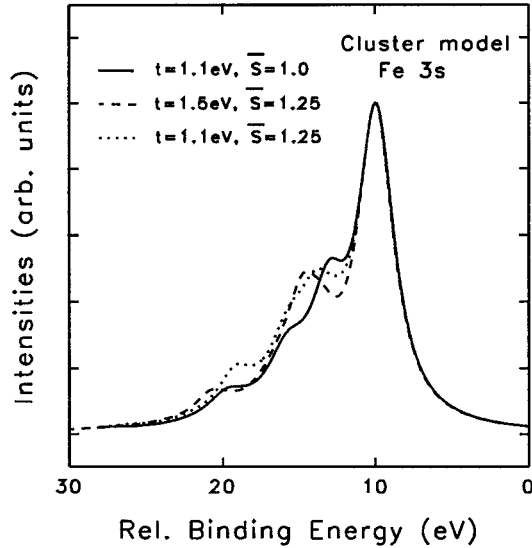
FIG. 7. Calculated spin integrated $3s$ spectra with various model parameters: (i) $\bar{S}$, $\bar{S}_z = 1.0$ eV, $t = 1.1$ eV, $U = 3.5$ eV, $J = 3.1$ eV, $Q = 3.5$ eV; (ii) $\bar{S}$, $\bar{S}_z = 1.25$, $t = 1.5$ eV, $U = 3.5$ eV, $J = 3.1$ eV, $Q = 3.5$ eV; (iii) $\bar{S}$, $\bar{S}_z = 1.25$, $t = 1.1$ eV, $U = 3.5$ eV, $J = 3.1$ eV, $Q = 3.5$ eV-.

FIG. 8. Analyses of spin-integrated $3s$ spectra under ferromagnetic ground state, 0.67, 1.67, and 2 ML thickness fcc thin films, $\bar{S}$, $\bar{S}_z = 1.0$, $t = 1.1$ eV, $U = 3.5$ eV, $J = 3.1$ eV, and $Q = 3.5$ eV. The dots and solid lines indicate experiment and theory, respectively.

see whether we can fit the $3s$ spectra of thin films or not. If J is invariant, the exchange splitting depends on the local magnetic moment directly in the atomic limit ($t = 0$). However, in our cluster model calculation, it is important to understand which parameter, t or $\bar{S}$, influence exchange splitting strongly. From varying the value of parameter selectively, we find that the peak-to-peak separation in the $3s$ spectra, so-called exchange splitting, depends on the local spin momentum $\bar{S}$ sensitively (Fig. 7). In addition to the peak separation, the intensity ratio between main and satellite peaks is also dependent upon the $\bar{S}$ parameter more strongly than the itinerancy t parameter. In the ultrathin films, the experimental exchange splitting is reduced to 4.0 eV from 4.6 eV of bulk bcc (Fig. 6). And the intensity ratio of the main and satellites changes from the bcc bulk to fcc films. Both facts imply the decrease of local magnetic moment from bcc bulk to fcc films judging from our model fitting. The decrease of Fe local moment in ultrathin Fe fcc films compared with bcc bulk has been also observed in neutron diffraction experiments.[35] We fitted the $3s$ spectra of fcc thin films with a four atomic cluster model having average spin $\bar{S} = 1.0$ (average local moment per atom $= 2.0\mu_B$) instead of average spin $\bar{S} = 1.25$ (average local moment per atom $= 2.5\mu_B$) for the bulk bcc iron. But in this case the total number of $3d$ electron was conserved as 28, so the average number of $3d$ electron per atom was 7, which is the same as in bcc bulk. From the model fitting (Fig. 8), we found that the experimental spectra can be fitted reasonably well with this assumption. As mentioned earlier the $3s$ spectra of thin films do not change appreciably depending on the thickness. The weak thickness dependence from 0.7 to 2 ML can be taken as evidence for similar local environment of Fe below 2 ML ultrathin fcc iron film on Cu(100). Our cluster calculation about ultrathin fcc films has been done under a ferromagnetic ground state scheme. This fact illustrates that the short range order of ultrathin fcc films is probably ferromagnetic.
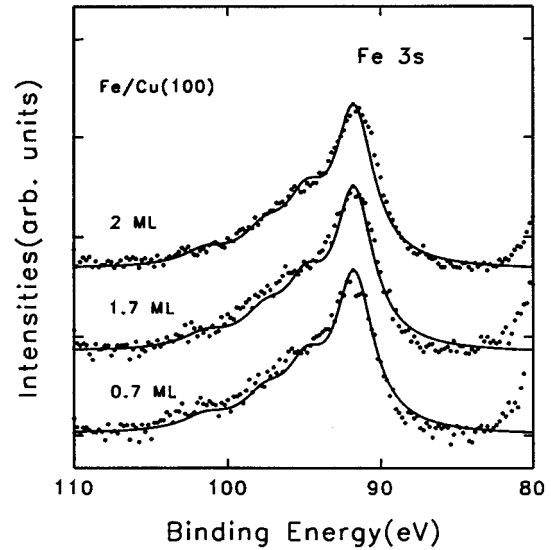
IV. CONCLUSION

We found that the $3s$ photoemission spectra of Fe bulk and fcc thin films can be understood from the cluster model calculation considering configuration interaction. From this cluster model approach of $3s$ spin integrated spectra, we found that the Fe local magnetic moment of fcc ultrathin film is reduced from that of bulk bcc Fe. In addition, the local magnetic moment below 2 ML thin films is nearly the same as ferromagnetic 2 ML thin film. This reveals that the absence of long range magnetic order below 2 ML is not due to the vanishing local magnetic moment.

*Electronic address: pkhidea.etri.re.kr

[1] L. M. Falicov *et al.*, J. Mater. Res. **5**, 1299 (1990).

[2] U. Gradmann, Appl. Phys. A **49**, 563 (1989).

[3] C. L. Fu, A. J. Freeman, and T. Oguchi, Phys. Rev. Lett. **54**, 2700 (1985).

[4] R. Richter, J. G. Gay, and J. R. Smith, Phys. Rev. Lett. **54**, 2704 (1985).

[5] D. Bagayoko and J. Callaway, Phys. Rev. B **28**, 5419 (1983).

[6] C. Liu, E. R. Moog, and S. D. Bader, J. Appl. Phys. **64**, 5325 (1988).

[7] J. Thomassen, F. May, B. Feldmann, M. Wuttig, and H. Ibach, Phys. Rev. Lett. **69**, 3831 (1992).

[8] R. Allenspach and A. Bischof, Phys. Rev. Lett. **69**, 3385 (1992).

[9] M. Stampanoni, A. Vaterlaus, M. Aeschlimann, F. Meier, and D. Pescia, J. Appl. Phys. **64**, 5321 (1988).

[10] Y. Darich, J. Marcano, H. Min, and P. A. Montano, Surf. Sci. **217**, 521 (1989).

[11] D. A. Steigerwald, I. Jacob, and W. F. Egelhoff, Jr., Surf. Sci. **202**, 472 (1988).

[12] M. T. Kief and W. F. Egelhoff, Jr., Phys. Rev. B **47**, 10 785 (1993).

[13] C. L. Fu and A. J. Freeman, Phys. Rev. B **35**, 925 (1987).

[14] J. Giergiel (unpublished).

[15] S. D. Healy, K. R. Heim, Z. Y. Yang, G. G. Hembree, J. S. Drucker, and M. R. Scheinfein, J. Appl. Phys. **75**, 5592 (1994).

[16] C. S. Fadley, D. A. Shirley, A. J. Freeman, P. S. Bagus, and J. V. Mallow, Phys. Rev. Lett. **23**, 1397 (1969).

[17] C. S. Fadley and D. A. Shirley, Phys. Rev. A **2**, 1109 (1970).

[18] P. S. Bagus, A. J. Freeman, and F. Sasaki, Phys. Rev. Lett. **30**, 850 (1973).

[19] J. H. Van Vleck, Phys. Rev. **45**, 405 (1934).

[20] J. F. van Acker, Y. M. Stadnik, J. C. Fuggle, H. J. W. Hoekstra, K. H. J. Buschow, and G. Stronik, Phys. Rev. B **37**, 6827 (1985).

[21] S.-J. Oh, G.-H. Gweon, and J.-G. Park, Phys. Rev. Lett. **68**, 2850 (1992); G.-H. Gweon, J.-G. Park, and S.-J. Oh, Phys. Rev. B **48**, 7825 (1993).

[22] Y. Kakehashi, K. Becker, and P. Fulde, Phys. Rev. B **29**, 16 (1984); Y. Kakehashi, *ibid.* **32**, 1607 (1985).

[23] C. Carbone, T. Kachel, R. Rochow, and W. Gudat, Solid State Commun. **77**, 619 (1991).

[24] F. U. Hillebrecht, R. Jungblut, and E. Kisker, Phys. Rev. Lett. **65**, 2450 (1990).

[25] T. Kachel, C. Carbone, and W. Gudat, Phys. Rev. B **47**, 15 391 (1993).

[26] E. Dagotto, R. Joynt, A. Moreo, S. Bacci, and E. Galiano, Phys. Rev. B **41**, 9049 (1990).

[27] E. Dagotto and A. Moreo, Phys. Rev. D **31**, 865 (1985).

[28] R. Haydock, V. Heine, and M. Kelly, J. Phys. C **5**, 2845 (1972); **8**, 2591 (1975).

[29] B. N. Cox, M. A. Coulthard, and P. Lloyd, J. Phys. F **4**, 807 (1974).

[30] D. van der Marel and G. A. Sawatzky, Phys. Rev. B **37**, 10 674 (1988).

[31] T. Bandyopadhyay and D. D. Sarma, Phys. Rev. B **39**, 3517 (1989).

[32] J. C. Slater, *Quantum Theory of Atomic Structure* (McGraw-Hill, New York, 1960).

[33] E. M. Heines, R. Clauberg, and R. Feder, Phys. Rev. Lett. **54**, 932 (1985).

[34] A. Kakizaki, H. Okuma, T. Kinoshita, A. Harasawa, and T. Ishii, Rev. Sci. Instrum. **63**, 367 (1992).

[35] W. Schwarzacher, W. Allison, R. F. Willis, J. Penfold, R. C. Ward, I. Jacob, and W. F. Egelhoff, Jr., Solid State Commun. **71**, 563 (1989).